

Heart Rate Sensing with a Robot Mounted mmWave Radar

Peijun Zhao[†], Chris Xiaoxuan Lu^{*†}, Bing Wang[†], Changhao Chen[†], Linhai Xie[†], Mengyu Wang[§],
Niki Trigoni[†], and Andrew Markham[†]

[†]Department of Computer Science, University of Oxford, United Kingdom

[§]Peking University, China

Abstract—Heart rate monitoring at home is a useful metric for assessing health e.g. of the elderly or patients in post-operative recovery. Although non-contact heart rate monitoring has been widely explored, typically using a static, wall-mounted device, measurements are limited to a single room and sensitive to user orientation and position. In this work, we propose **mBeats**, a robot mounted millimeter wave (mmWave) radar system that provide periodic heart rate measurements under different user poses, without interfering in a users daily activities. **mBeats** contains a mmWave servoing module that adaptively adjusts the sensor angle to the best reflection profile. Furthermore, **mBeats** features a deep neural network predictor, which can estimate heart rate from the lower leg and additionally provides estimation uncertainty. Through extensive experiments, we demonstrate accurate and robust operation of **mBeats** in a range of scenarios. We believe by integrating mobility and adaptability, **mBeats** can empower many downstream healthcare applications at home, such as palliative care, post-operative rehabilitation and telemedicine.

I. INTRODUCTION

Heart rate monitoring is a key indicator for assessing health, stress and fitness. In particular, periodic (e.g. hourly) monitoring of elderly patients, those in palliative care, or patients undergoing post-operative rehabilitation provides a quantifiable metric of whether intervention from a health professional is required or not [1]. This is increasingly important as there is an increasing shift towards caring for patients within their homes, rather than in hospitals, as it is more cost-effective [2].

Significant strides have been made in ambulatory heart rate monitoring e.g. with wearable devices operating either with electrocardiogram (ECG) or photoplethysmography (PPG) sensors. In particular, smart-watches and fitness bands provide a ‘wear and forget’ capability and have made continuous heart rate monitoring inexpensive and wide-spread. Although wearables are an excellent solution for the general public, for the aforementioned problems they suffer from ‘forget to wear’ and ‘forget to charge’ issues. This leads to low compliance, making them unsuitable for monitoring patients with physical or mental health issues. Alternatives include sensor-equipped beds [3] but these are limited to monitoring patients in a single location.

These limitations have lead to the development of non-contact heart rate monitoring solutions, including those based on imaging and radio-frequency (RF) techniques. With respect to the former, a camera (either in the visible or infrared



Fig. 1: **mBeats** is a robot mounted mmWave radar system. It is able to provide periodic heart rate measurements of a user, without interfering in a user’s daily activities, and without being constrained to only operate at a certain location.

spectrum) is used to detect subtle variations in blood vessel dilation in the face [4]. These require a direct line-of-sight to the patient, and do not work with occlusions e.g. clothing. They also raise issues about privacy, due to the use of cameras. RF based techniques operate by inferring the micro-displacement of the heart through subtle changes in the reflected radio signal. Most work to date has considered using a static device e.g. placed on a wall, to obtain these measurements [5], [6]. However, these types of sensors are very sensitive to the orientation and position of a user [7].

An ideal system, as shown in Fig. 1, would be able to provide periodic heart rate measurements of a user, without requiring anything to be worn, and without being constrained to only operate at a certain location. Motivated by the increasing adoption of domestic service robots e.g. robotic vacuum cleaners, we posit a scenario where these could serve a dual purpose as mobile heart rate scanners. We in particular exploit recent developments in the miniaturization of single-chip, low-cost (<\$100) mmWave radar which is capable of accurately measuring micron-level displacements. We believe it is quite likely that low-cost robotic platforms of the future will be equipped with mmWave radar for obstacle avoidance [8]. In this way, a domestic service robot could periodically scan a patient’s heart rate before continuing with its normal operation.

In this paper, we present **mBeats**, a novel approach towards providing non-contact heart rate measurements throughout the home, without requiring any fixed infrastructure or compliance with charging and wearing a device. A particular challenge is that service robots are typically low in height and close to the floor and thus unable to sense the heart itself. Instead, we demonstrate that it is possible, by using mmWave radar, to measure the heart rate in a user’s lower leg, operating through clothing. This is a diffi-

*Corresponding author: Chris Xiaoxuan Lu (xiaoxuan.lu@cs.ox.ac.uk)

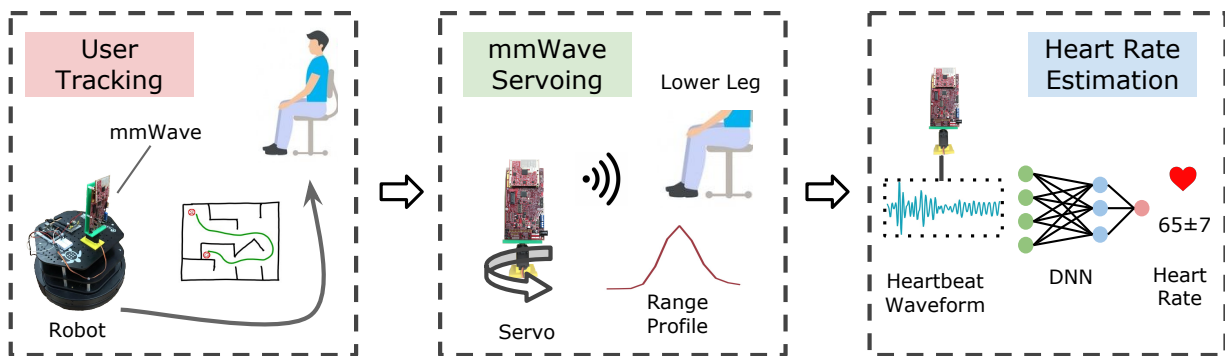


Fig. 2: mBeats consists of three modules operating in a pipelined manner. (i) *user tracking module* actively tracks a target with the mmWave radar and instructs the mobile robot to move towards the user’s proximity; (ii) *mmWave servoing module* adaptively rotates the mmWave radar that optimises the sensor angle for best heart rate observation; and (iii) *heart rate estimation module* senses the micro displacement of user’s skin and estimates his heart rate with a confidence interval.

cult signal processing challenge as the radar return is very small. To solve it we rely on advances in deep learning to extract accurate heart rate measurements. Unlike competing approaches, not only do we provide a measurement, we also provide a metric of uncertainty. This is critical for providing trustworthy measurements without creating false alarms, or worse, not reflecting an emergency condition.

The main contributions of this work are:

- To the best of our knowledge, this is the first work to implement robot based heart rate measurement with mmWave Radar.
- We propose a feedback control approach to actively steer the mmWave radar for optimal signal detection.
- We use a deep neural network to process the radar displacement measurements to accurately measure the heart rate in the lower leg. This network can provide estimation uncertainty proportional to prediction errors.
- We release the implementation of mBeats to the community, including code and datasets.

II. RELATED WORK

In this section, we review non-contact based heart rate monitoring techniques.

A. Electrocardiogram-based Techniques

Non-contact Electrocardiogram measuring uses capacitive electrodes instead of the conventional adhesive electrodes, and thus do not have to be in contact with the user’s skin directly. These kind of sensors have been embedded in a range of different objects, e.g. a bed [9], wheelchair [10], driver’s seats [11], etc. Although far less intrusive than conventional electrode-based ECG, it requires the user to be very close (a few cm) to the sensor, limiting its applicability.

B. Vision-based Techniques

Vision-based Heart Rate Measuring has been widely researched. In most of these methods, a Region of Interest is first detected and tracked, over various parts of the body [4], [12], [13]. As the heart beats, blood flow causes subtle color

changes on human skin and this information can be captured with an RGB camera. Infrared cameras have also been used for heart rate detection [12], [14], [15], and can even extract heart beat information from pupillary fluctuations [16]. Vision-based techniques can work well for tasks like sleep monitoring [17], or telemedicine with a webcam [18], and puts least burden on the user. However, they can only work under line-of-sight conditions and raise privacy issues. RGB based systems also are typically restricted to well illuminated conditions.

C. RF-based Techniques

RF-based heart rate measuring techniques are primarily based on Radar and WiFi. Various types of radar like UWB Impulse Doppler Radar [19], Continuous Wave Radar [20], and Frequency-Modulated Continuous Wave Radar [5], with different operating frequencies and output powers have been used for this scenario. These techniques measure the micro-displacement of a user’s skin. Radar signals can penetrate many kinds of materials so can perform non-line-of-sight measuring of vital signs. However, signal strength impacts the operation range, with consequent trade-off between transmitter power and measurement distance [21].

WiFi-based techniques are widely used for RF-based heart rate measuring, as most of these techniques can be implemented with commercial-off-the-shelf WiFi devices, like routers and laptops. Micro-displacement of the user’s skin is estimated by capturing the channel state information (CSI) [22], [23]. However, the accuracy of WiFi-based techniques is greatly affected by the user’s location and body orientation [7].

The aforementioned techniques are mainly based on conventional signal processing algorithms, like Fast-Fourier Transform, Auto-correlation, etc. These algorithms have long been used to extract periodic information from time series signals.

Our approach broadly falls into this category of RF based monitoring, however, has three prominent advantages over other methods. The first is that by mounting the system

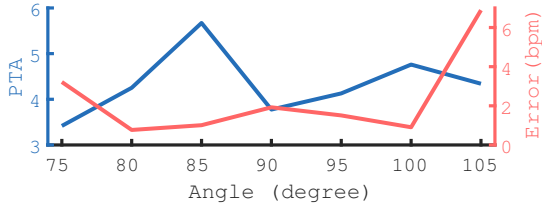


Fig. 3: Impact of observation angles on heart rate estimation. We place the robot approximately 0.5m away from a user’s lower leg and rotate the sensor from 75° to 105° at a stride of 5° and each angle for approximately 40 seconds. The error is obtained from a fixed estimation method [26]. PTA: Peak-to-Average ratio.

on a low-height mobile robot, our approach is location independent. Secondly, we are able to measure the heart rate in the lower leg, by using the high displacement sensitivity of mmWave radar, making the system non-intrusive i.e. it does not need to be at chest height. Lastly, as our experimental results show, compared to the conventional methods based on signal processing algorithms and heuristics, our system reaches the highest accuracy.

III. PROPOSED SYSTEM

mBeats comprises of a robotic platform equipped with a mechanically steerable mmWave radar module. Without loss of generality, in our work we use a TI IWR6843 single chip mmWave radar, which operates by sending out a frequency modulated continuous wave (FMCW) chirp over a 4 GHz bandwidth, centred on 62 GHz. By measuring the time for the signal to return to a colocated antenna and correlating with the transmitted signal, it is possible to measure the range to reflective objects with high accuracy (cm level). By computing the phase difference between successive scans, it is then possible to measure relative displacements with near micron-level accuracy [24].

The three modules in our active sensing and signal processing pipeline are shown in Fig. 2, including (i) user tracking, (ii) mmWave servoing and (iii) heart rate estimation.

A. User Tracking Module

The user tracking module is largely based on [25] that utilizes the mmWave point cloud to pinpoint the user in the field of view. Given the estimated user’s location, a robot then approaches the user at a certain measurement distance (0.5m in this work), and performs subsequent sensing actions. As this is not our primary contribution, we assume in the remainder of the paper that the robot can localize and approach a person to be scanned.

B. mmWave Servoing Module

Unlike a planar surface, directly facing the user does not guarantee the best reflection signal, as the tibia and fibula bones in the calf block the signal. Furthermore, due to multi-path effects caused by surrounding objects, a small deviation from the optimal direction may lead to a significantly degraded performance. As such, given a good measurement

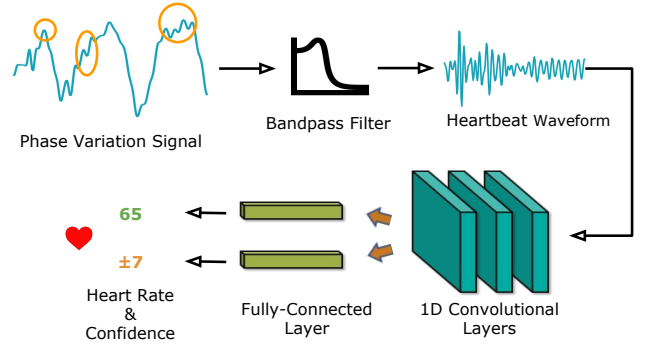


Fig. 4: Heart Rate Estimation. A bandpass filter is used to extract heartbeat waveforms (circled in orange) from phase variation signals. A convolutional neural network takes inputs as the extracted waveforms and predicts both a heart rate value and a confidence interval.

distance, the heart rate estimation accuracy of a mmWave radar still largely depends on observation angles (see Fig. 3).

The goal of this module is therefore to optimise the sensor angle for peak signal reflection from the patient’s lower leg/calf. Although it would be possible to rotate the robot itself, depending on the capabilities of current service robots, this is cumbersome and would be imprecise to reach the optimal angle. Hence we control the orientation of sensor with a *servo motor* directly according to the characteristics of the reflected mmWave signal.

Formally, we take the desired change of the measurement angle $\Delta\theta$ as the control variable u_t at time t . Next, based on the Peak To Average (PTA) value v_t provided from the sensor which indicates the reflected signal strength, we define the observation variable as

$$y_t = -\text{sgn}(u_{t-1})(v_t - v_{t-1}), \quad (1)$$

where $\text{sgn}(x) = \frac{|x|}{x}$ if $x \neq 0$ else $\text{sgn}(x) = 0$ and $u_0 = 1^\circ$. This observation function uses the direction of the prior control variable u_{t-1} and the change of the received signal strength as the feedback for our control system. Then, given a zero reference $r_t = 0$, the error variable is obtained as:

$$e_t = r_t - y_t = \text{sgn}(u_{t-1})(v_t - v_{t-1}), \quad (2)$$

with the intuition that we vary the orientation of the sensor towards the prior direction when observing an increased signal strength and vice-versa. We use a simple Proportional-Derivative (PD) controller with the following feedback control function:

$$u_t = u_{t-1} + K_p \cdot e_t + K_d \cdot (e_t - e_{t-1}) \quad (3)$$

where K_p and K_d are empirically set to 3.6 and 1.8. As the heart rate measurement requires a static measuring environment, we disable the PD controller when the error variable e_t has settled.

C. Heart Rate Estimation Module

1) *Heartbeat Waveform Extraction*: After rotating the sensor to the optimal orientation, the mmWave radar starts to sense the micro displacement of the user’s skin by measuring the phase variation respective to the range profile peak. Nevertheless, in addition to heartbeat waveforms, the phase variation also contains signals caused by other body movements that may lead to erroneous estimation. Considering the fact that heartbeat frequency lies in the band between $0.8 \sim 4\text{Hz}$ [5], we leverage a biquad cascade IIR filter [27] in this module to extract heartbeat waveforms. The extracted waveforms are then used as inputs for next module.

2) *DNN Predictor*: Unlike prior work where the sensor is facing a user’s chest, our mmWave radar collects signals from lower legs. For each heart beat, the chest usually has a vibration amplitude of 400 micron, while the displacement of the skin on lower leg only has an amplitude of around 80 micron. Consequently, the collected signals are much weaker and our extracted heartbeat waveforms have much less clear patterns than prior art. Directly using these waveforms to predict heart rate e.g. through peak extraction is difficult and error-prone. Deep neural networks have recently emerged as a powerful data-driven technique, effective at learning latent features in data. We therefore formulate heart rate estimation as a regression problem, and use a convolution neural network as the predictor. Although RNN networks, e.g., Long-Short Term Memory networks (LSTM), are widely used for modeling temporal signals, such as reconstructing pedestrian trajectories from IMU data [28], their recursive computation incurs substantial latency [29] that cannot provide timely predictions on our resource-constrained platforms. Given this real-time consideration, our network adopts three lightweight 1-D convolutional layers, followed by two fully connected layers to produce heart rate and uncertainty respectively. In particular, the number of kernels, kernel sizes and strides of all convolution layers are set to 64, 5 and 1 respectively. By taking inputs as the heartbeat waveforms with a window size of 10 seconds (200 frames), the predictor is able to provide both rate value and confidence interval (in the form of uncertainty). Fig. 4 illustrates this process.

DNN Predictor transforms the signal input $\mathbf{x} \in \mathbb{R}^{200 \times 1}$ (heartbeat waveform) into predicted heart rate $\hat{\mathbf{y}} = f^{\mathbf{W}}(\mathbf{x}) \in \mathbb{R}^1$ with model parameters \mathbf{W} (i.e. weights, bias in neural networks). Typically, the optimal parameters are recovered by minimizing the mean square error (MSE) loss between the prediction and ground truth \mathbf{y} :

$$\text{loss}(\mathbf{x}) = \|\mathbf{y} - \hat{\mathbf{y}}\|_2, \quad (4)$$

The output $\hat{\mathbf{y}}$ only reflects the mean value of prediction given input data with corresponding labels. We will show how to extend this framework to a Bayesian model to capture output uncertainty in next subsection.

3) *Uncertainty Estimation*: Although heart rate regression with a DNN is relatively straightforward, uncertainty estimation is non-trivial. The uncertainty reflects to what extent the predicted heart rates can be trusted. This is extremely

critical to health-related problems, as wrong values will lead to serious consequences, e.g., misdiagnosis. Intuitively, the uncertainties in our problem are originated from inaccurate mmWave measurements, due to sensor biases and noises, environmental dynamics, multipath reflection and non-optimal reflection plane. We hence quantify the uncertainty of our model based on the aleatoric uncertainty which is widely used to capture inherent sensor observation noise [30], [31].

In order to estimate the uncertainty of predicted heart rates, we reformulate Equation 4 into a Bayesian model by defining the likelihood between the prediction $f^{\mathbf{W}}(\mathbf{x})$ and ground truth \mathbf{y} as a conditional probability following a Gaussian distribution:

$$p(\mathbf{y}|f^{\mathbf{W}}(\mathbf{x})) = \frac{1}{\sqrt{2\pi\sigma^2}} \exp\left(-\frac{(\mathbf{y} - f^{\mathbf{W}}(\mathbf{x}))^2}{2\sigma^2}\right), \quad (5)$$

where σ^2 denotes the prediction variance. To maximize the likelihood $p(\mathbf{y}|f^{\mathbf{W}}(\mathbf{x}))$, we need to determine an optimal set of parameters \mathbf{W}^* , which can be achieved by minimizing the negative logarithm likelihood $\log p(\mathbf{y}|f^{\mathbf{W}}(\mathbf{x}))$:

$$\begin{aligned} \mathbf{W}^* &= \arg \max_{\mathbf{W}} p(\mathbf{y}|f^{\mathbf{W}}(\mathbf{x})) \\ &= \arg \min_{\mathbf{W}} -\log p(\mathbf{y}|f^{\mathbf{W}}(\mathbf{x})) \\ &= \arg \min_{\mathbf{W}} \frac{1}{2\sigma^2} \|\mathbf{y} - f^{\mathbf{W}}(\mathbf{x})\|_2^2 + \frac{1}{2} \log \sigma^2. \end{aligned} \quad (6)$$

Thus, we can define the loss function of the model as

$$\text{loss}(\mathbf{x}) = \frac{\|\mathbf{y} - \hat{\mathbf{y}}\|_2^2}{2\sigma^2} + \frac{1}{2} \log \sigma^2 \quad (7)$$

where the model predicts a mean $\hat{\mathbf{y}}$ and variance σ^2 . From this loss function, we can see that poor predictions will encourage the network to decrease the residual term, by increasing uncertainty σ^2 . On the contrary, the term $\log \sigma^2$ acts to prevent the unbounded growth of the uncertainty term. In practice, we aim to learn $\mathbf{s} = \log \sigma^2$ as it is more numerically stable [32] in this way:

$$\text{loss}(\mathbf{x}) = \frac{\|\mathbf{y} - \hat{\mathbf{y}}\|_2^2}{2 \exp(\mathbf{s})} + \frac{1}{2} \mathbf{s}. \quad (8)$$

IV. IMPLEMENTATION

For the purpose of reproducing our approach, we release a novel dataset of mmWave heart rate measurement and our source code of neural networks: <https://github.com/zhaoymn/mbeats>.

A. Data Collection

1) *Collection System*: We installed the mmWave radar sensor on a Turtlebot 2 [33]. A commercial servo motor is installed on the robot platform as well and we use it to precisely control the radar rotation in 1° . The servo control unit is implemented by Arduino Uno [34]. Concerning the mmWave radar, we adopt the IWR6843 ISK [35], which is an emerging low-cost single-chip sensor. Both mmWave data and timestamps are logged. Polar H10, an accurate heart rate monitor chest strap is used in our experiment for ground truth labelling. An Android application is developed to record



Fig. 5: The 8 different poses used in test and evaluation.

Polar H10 heart rate data and timestamps via Bluetooth. We will release this Android Application for community use. The data from the radar and the data from the Polar H10 device are synchronized to the same NTP time.

2) *Selected Poses*: According to the American Time Use Survey released in June, 2019 [36], people spend 12.61 hours on average either sitting or lying down/sleeping at home each day, accounting for over 50% of time in a day and over 80% of time at home. We thus select four different sitting poses and different lying poses at home in our data collection (see Fig. 5). We collect ~ 180 minutes of data from two subjects in these poses.

B. Network Training

To train the proposed network, we set the window size to 10s, which consists of 200 frames as the input data. The uncertainty component in our network is initialized with zeros, while the remaining parts are randomly initialized. The network is implemented with PyTorch, applying the ADAM optimizer with a constant learning rate of 1×10^{-5} . The network is trained on a NVIDIA Titan X GPU with a mini-batch size of 512 and a dropout rate probability of 0.2.

V. EVALUATION

In this section, we systematically evaluate `mBeats`. We start with the introduction of experiment setup and then compare our DNN predictor with established baselines for heart rate estimation. Uncertainty estimation is examined, followed by studying the impacts of the servoing module.

A. Setup

1) *Competing Approaches*: In this section, three common signal processing approaches are used as the baseline approaches: Fast Fourier Transform (FFT) [26], Peak Count (PK) [37] and Auto-correlation (XCORR) [38].

2) *Pre-processing*: After obtaining the raw data stream, frames in the first 40 seconds and in the last 20 seconds are discarded due to system calibration. Additionally, data frames collected while the mmWave servoing module is dynamically searching for best orientation are also discarded. We take samples with a sliding window with a size of 200 and stride of 1.

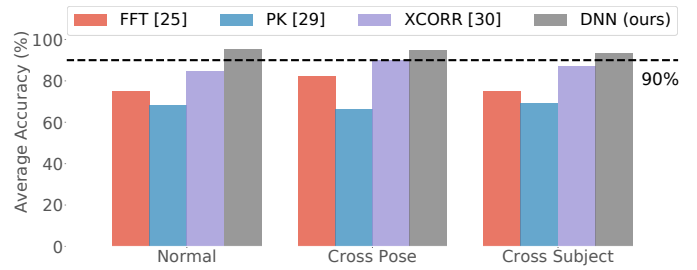


Fig. 6: Overall performance comparison in different test categories. The 90% accuracy line is indicated for reference.

TABLE I: Holistic Evaluation Results.

	FFT [26]	PK [37]	XCORR [38]	DNN (Ours)
Pose 1	77.02	65.84	91.95	97.89
Pose 2	89.94	65.88	88.49	96.11
Pose 3	52.43	75.70	48.27	93.76
Pose 4	83.18	73.41	92.67	96.97
Pose 5	93.46	64.31	94.10	94.85
Pose 6	74.59	67.81	85.89	94.75
Pose 7	64.35	64.22	91.06	91.08
Pose 8	74.57	70.60	87.24	96.64
Overall	76.19	68.47	84.96	95.26

3) *Evaluation Protocol*: Similar to [5], we use *accuracy* as the evaluation metric throughout our experiments. It is worth mentioning that, for clinical validity [39], a usable heart rate estimator should have at least 90% accuracy. For training our DNN predictor, we split our data into training, validation and test sets. The three sets are prepared differently according to the experiment requirements, which will be detailed in subsequent sections.

B. Performance Comparison

To validate the heart rate estimation accuracy and robustness of our DNN predictor, three experiments are carried out, including (i) holistic evaluation on all poses, (ii) cross pose evaluation, and (iii) cross subject evaluation. Fig. 6 summarizes the overall comparison results.

1) *Holistic Comparison*: In this experiment, all data streams are equally divided into 5 continuous segments where segments 1,3,5 are for as training whilst segment 4 and segment 2 are used for validation and testing respectively.

As shown Tab. I, although the competing methods have previously been shown to be effective for chest-sensing scenario, they struggle to accurately estimate heart rate when it comes to lower-leg sensing. Because the sensed micro skin displacement is very weak from the calf, the competing approaches cannot reliably estimate the heart rate and be consistently accurate across different poses. For instance, as the best-performing baseline, XCORR achieves a 94.10% accuracy on Pose 5, but its accuracy on Pose 3 is as low as 48.27%. The low robustness of XCORR makes it unsuitable to real domestic scenarios where diverse daily poses are common. When considering the 90% accuracy standard to measure method efficacy, our proposed DNN estimator is the only approach that meets this under all 8 poses, with a 5.26% safety margin overall. In contrast, FFT method only

TABLE II: Cross Pose Test Result

	FFT [26]	PK [37]	XCORR [38]	DNN (Ours)
Pose 2	91.90	63.69	91.30	96.08
Pose 6	72.61	69.36	88.87	93.94

TABLE III: Cross Subject Test Result

	FFT [26]	PK [37]	XCORR [38]	DNN (Ours)
Subject 1	75.38	72.99	83.61	93.85
Subject 2	75.13	65.73	90.36	93.03

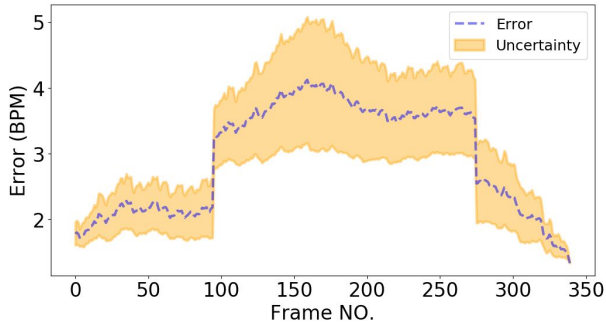


Fig. 7: Uncertainty Estimation. The estimated uncertainty is informative that increases with prediction errors.

attains this accuracy in one pose, while PK fails to achieve this standard under all poses.

2) *Cross Pose Evaluation*: We next evaluate the generalization ability of our DNN estimator across different poses. To this end, we split the dataset into 8 segments corresponding to the different poses. The data with Pose 1,3,5,7 are used as the training data, Pose 4 and 8 for model validation purpose, and Pose 2 and 6 as testing data.

As we can see in Tab. II, our DNN approach has a strong generalization ability w.r.t. different user poses, giving 96.08% and 93.94% accuracy on the unseen data from Pose 2 and 6. The accuracy drop from holistic testing to cross pose is only 0.25%, indicating the feasibility for real world deployment. Notably, FFT, PK and XCORR are signal processing based methods and in principle insensitive to cross poses. However, their accuracy is still inferior to our DNN estimator.

3) *Cross Subject Evaluation*: We further evaluate our method on cross subject testing, where the DNN estimator is tested on the data collected from a new subject outside the training set.

Although different people have different heartbeat patterns [40], [41], as we can see in Tab. III, our DNN estimator still yields a testing accuracy of 93.85% and 93.03% on two different subjects respectively. Such high accuracy significantly outperforms competing approaches by $\sim 7\%$. This generalisation ability is of paramount importance for real world deployment, as a crowd-sourcing approach can be used to train the DNN predictor before shipping to customers.

C. Uncertainty Evaluation

As described in Sec. III-C.3, our method has a prominent advantage in that is capable of providing a confidence

TABLE IV: The overall performance with and without the mmWave servoing module.

	FFT [26]	PK [37]	XCORR [38]	DNN (Ours)
w.o. Servoing (PTA=2.11)	78.71	75.90	62.43	90.71
w. Servoing (PTA=3.27)	80.74	88.77	87.61	92.20

estimation alongside the heart rate prediction. This is important for avoiding false alarms during healthcare monitoring where predictions with high uncertainty can be filtered out. Besides, it also acts as a clue towards improving the network by learning with more samples in undertrained situations, important for life-long learning.

Fig. 7 demonstrates an example of uncertainty estimation in the *cross pose* experiment. We can see a positive correlation between the uncertainty, i.e. the variation, and the prediction error. More specifically, we observed small variation (< 0.5) when the error is below 3 BPM, while the variation can reach 1.2 at peak error.

D. Impact of the mmWave Servoing Module

In the prior experiments, we used heartbeat waveforms collected with the optimal observing view. In the last experiment, we investigate the importance of incorporating the mmWave servoing module into the system loop, which is responsible for searching the optimal observing view.

We collected a 3-minute data stream twice with the same user pose and robot position. The only difference is whether the servo module is used or not. Note that the initial measuring view of the mmWave radar is manually set to deg 75, deviating from the optimal angle. To have a fair comparison, we fix this initialization setup for all baseline testing. From the experimental results in Tab. IV, we can see that with the mmWave Servoing module turned on, the PTA metric is improved from an average of 2.11 to an average of 3.27. This in turn enhances the overall measuring accuracy of all methods. This is consistent with our hypothesis that PTA is vital to measurement accuracy and consequently proves the necessity of utilising a mmWave servoing module for direction optimization before measurements.

Moreover, our method, once again, shows superior performance on the task. Even if the mmWave Servoing module is disabled, our method is still the only method that produces a satisfactory accuracy of over 90%, demonstrating a strong generalisation ability in unseen scenarios.

VI. CONCLUSION

In this work, we proposed mBeats, a robot mounted mmWave radar system that provides periodic heart rate measurements under diverse poses without intruding on a users daily activities. mBeats demonstrated, through the use of a novel deep-learning approach, how accurate heart rate measurements could be obtained from the lower-leg, with corresponding uncertainty estimates. Future work will consider how to measure heart rate from a moving subject, a current limitation of our technique where locomotion signals swamp the weak heart rate signals, and to train with a larger number of participants.

REFERENCES

- [1] M. Ishijima, "Cardiopulmonary monitoring by textile electrodes without subject-awareness of being monitored," *Medical and Biological Engineering and Computing*, vol. 35, no. 6, pp. 685–690, 1997.
- [2] D. A. Perednia and A. Allen, "Telemedicine technology and clinical applications," *Jama*, vol. 273, no. 6, pp. 483–488, 1995.
- [3] Z. Jia, A. Bonde, S. Li, C. Xu, J. Wang, Y. Zhang, R. E. Howard, and P. Zhang, "Monitoring a person's heart rate and respiratory rate on a shared bed using geophones," in *Proceedings of the 15th ACM Conference on Embedded Network Sensor Systems*, 2017.
- [4] S. Tulyakov, X. Alameda-Pineda, E. Ricci, L. Yin, J. F. Cohn, and N. Sebe, "Self-adaptive matrix completion for heart rate estimation from face videos under realistic conditions," in *Proceedings of the IEEE Conference on Computer Vision and Pattern Recognition*, 2016, pp. 2396–2404.
- [5] F. Adib, H. Mao, Z. Kabelac, D. Katabi, and R. C. Miller, "Smart homes that monitor breathing and heart rate," in *Proceedings of the 33rd annual ACM conference on human factors in computing systems*. ACM, 2015, pp. 837–846.
- [6] M. Zhao, F. Adib, and D. Katabi, "Emotion recognition using wireless signals," in *Proceedings of the 22nd Annual International Conference on Mobile Computing and Networking*. ACM, 2016, pp. 95–108.
- [7] H. Wang, D. Zhang, J. Ma, Y. Wang, Y. Wang, D. Wu, T. Gu, and B. Xie, "Human respiration detection with commodity wifi devices: do user location and body orientation matter?" in *Proceedings of the 2016 ACM International Joint Conference on Pervasive and Ubiquitous Computing*. ACM, 2016, pp. 25–36.
- [8] S. Sugimoto, H. Tateda, H. Takahashi, and M. Okutomi, "Obstacle detection using millimeter-wave radar and its visualization on image sequence," in *International Conference on Pattern Recognition*, 2004.
- [9] M. Wong, E. Pickwell-MacPherson, and Y. Zhang, "Contactless and continuous monitoring of heart rate based on photoplethysmography on a mattress," *Physiological measurement*, vol. 31, no. 7, p. 1065, 2010.
- [10] B. Chamadiya, K. Mankodiya, M. Wagner, and U. G. Hofmann, "Textile-based, contactless eeg monitoring for non-icu clinical settings," *Journal of Ambient Intelligence and Humanized Computing*, vol. 4, no. 6, pp. 791–800, 2013.
- [11] B. Eilebrecht, T. Wartzek, J. Lem, R. Vogt, and S. Leonhardt, "Capacitive electrocardiogram measurement system in the driver seat," *ATZ worldwide eMagazine*, vol. 113, no. 3, pp. 50–55, 2011.
- [12] M. N. H. Mohd, M. Kashima, K. Sato, and M. Watanabe, "A non-invasive facial visual-infrared stereo vision based measurement as an alternative for physiological measurement," in *Asian Conference on Computer Vision*. Springer, 2014, pp. 684–697.
- [13] K.-Z. Lee, P.-C. Hung, and L.-W. Tsai, "Contact-free heart rate measurement using a camera," in *2012 Ninth Conference on Computer and Robot Vision*. IEEE, 2012, pp. 147–152.
- [14] K. Bakhtiyari, N. Beckmann, and J. Ziegler, "Contactless heart rate variability measurement by ir and 3d depth sensors with respiratory sinus arrhythmia," *Procedia Computer Science*, vol. 109, pp. 498–505, 2017.
- [15] X. He, R. Goubran, and F. Knoefel, "Ir night vision video-based estimation of heart and respiration rates," in *2017 IEEE Sensors Applications Symposium (SAS)*. IEEE, 2017, pp. 1–5.
- [16] A. Parnandi and R. Gutierrez-Osuna, "Contactless measurement of heart rate variability from pupillary fluctuations," in *2013 Humaine Association Conference on Affective Computing and Intelligent Interaction*. IEEE, 2013, pp. 191–196.
- [17] M. H. Li, A. Yadollahi, and B. Taati, "Noncontact vision-based cardiopulmonary monitoring in different sleeping positions," *IEEE journal of biomedical and health informatics*, vol. 21, no. 5, pp. 1367–1375, 2016.
- [18] M.-Z. Poh, D. J. McDuff, and R. W. Picard, "Advancements in non-contact, multiparameter physiological measurements using a webcam," *IEEE transactions on biomedical engineering*, vol. 58, no. 1, pp. 7–11, 2010.
- [19] L. Ren, Y. S. Koo, H. Wang, Y. Wang, Q. Liu, and A. E. Fathy, "Noncontact multiple heartbeats detection and subject localization using ubw impulse doppler radar," *IEEE Microwave and Wireless Components Letters*, vol. 25, no. 10, pp. 690–692, 2015.
- [20] J. Salmi, O. Luukkonen, and V. Koivunen, "Continuous wave radar based vital sign estimation: Modeling and experiments," in *2012 IEEE Radar Conference*. IEEE, 2012, pp. 0564–0569.
- [21] J. Kranjec, S. Beguš, G. Geršak, and J. Drnovšek, "Non-contact heart rate and heart rate variability measurements: A review," *Biomedical signal processing and control*, vol. 13, pp. 102–112, 2014.
- [22] X. Wang, C. Yang, and S. Mao, "Phasebeat: Exploiting csi phase data for vital sign monitoring with commodity wifi devices," in *2017 IEEE 37th International Conference on Distributed Computing Systems (ICDCS)*. IEEE, 2017, pp. 1230–1239.
- [23] J. Liu, Y. Wang, Y. Chen, J. Yang, X. Chen, and J. Cheng, "Tracking vital signs during sleep leveraging off-the-shelf wifi," in *Proceedings of the 16th ACM International Symposium on Mobile Ad Hoc Networking and Computing*. ACM, 2015, pp. 267–276.
- [24] T. Instruments, "MMWave Training Series," <https://training.ti.com/mmwave-training-series>.
- [25] P. Zhao, C. X. Lu, J. Wang, C. Chen, W. Wang, N. Trigoni, and A. Markham, "mid: Tracking and identifying people with millimeter wave radar," in *International Conference on Distributed Computing in Sensor Systems*, 2019.
- [26] L. Anitori, A. de Jong, and F. Nennie, "Fmcw radar for life-sign detection," in *2009 IEEE Radar Conference*. IEEE, 2009, pp. 1–6.
- [27] T. Kwan and K. Martin, "Adaptive detection and enhancement of multiple sinusoids using a cascade iir filter," *IEEE Transactions on Circuits and Systems*, vol. 36, no. 7, pp. 937–947, 1989.
- [28] C. Chen, P. Zhao, C. X. Lu, W. Wang, A. Markham, and N. Trigoni, "Deep learning based pedestrian inertial navigation: Methods, dataset and on-device inference," *IEEE Internet of Things Journal*, 2020.
- [29] C. X. Lu, B. Du, P. Zhao, H. Wen, Y. Shen, A. Markham, and N. Trigoni, "Deepauth: in-situ authentication for smartwatches via deeply learned behavioural biometrics," in *Proceedings of the 2018 ACM International Symposium on Wearable Computers*, 2018.
- [30] A. Kendall and Y. Gal, "What uncertainties do we need in bayesian deep learning for computer vision?" in *Advances in neural information processing systems*, 2017, pp. 5574–5584.
- [31] C. Chen, X. Lu, J. Wahlstrom, A. Markham, and N. Trigoni, "Deep neural network based inertial odometry using low-cost inertial measurement units," *IEEE Transactions on Mobile Computing*, 2019.
- [32] A. Kendall, Y. Gal, and R. Cipolla, "Multi-task learning using uncertainty to weigh losses for scene geometry and semantics," in *Proceedings of the IEEE Conference on Computer Vision and Pattern Recognition*, 2018, pp. 7482–7491.
- [33] "Turtle Bot 2," <https://www.turtlebot.com/turtlebot2/>.
- [34] "Arduino," <https://www.arduino.cc>.
- [35] T. Instruments, "TI IWR6843ISK," <http://www.ti.com/tool/IWR6843ISK>.
- [36] "American Time Use Survey News Release," <https://www.bls.gov/news.release/atus.htm>.
- [37] D. J. Ewing, J. Neilson, and P. Travis, "New method for assessing cardiac parasympathetic activity using 24 hour electrocardiograms," *Heart*, vol. 52, no. 4, pp. 396–402, 1984.
- [38] M. Sekine and K. Maeno, "Non-contact heart rate detection using periodic variation in doppler frequency," in *2011 IEEE Sensors Applications Symposium*. IEEE, 2011, pp. 318–322.
- [39] F. Sartor, G. Papini, L. G. E. Cox, and J. Cleland, "Methodological shortcomings of wrist-worn heart rate monitors validations," *Journal of medical Internet research*, vol. 20, no. 7, p. e10108, 2018.
- [40] S. A. Israel, J. M. Irvine, B. K. Wiederhold, and M. D. Wiederhold, *The heartbeat: the living biometric*. Wiley-IEEE Press, New York, NY, USA, 2009.
- [41] C. Hegde, H. R. Prabhu, D. Sagar, P. D. Shenoy, K. Venugopal, and L. M. Patnaik, "Heartbeat biometrics for human authentication," *Signal, Image and Video Processing*, vol. 5, no. 4, p. 485, 2011.